Removal of copper(II) ion from aqueous solution by high-porosity activated carbon

Dragan D Milenković[1], Milutin M Milosavljević[2], Aleksandar D Marinković[3], Veljko R Đokić[3], Jelena Z Mitrović[4] and Aleksandar Lj Bojić[4*]

[1]High Chemical Technological School, Department of Chemical Technology, Kosančićeva 36, 37000 Kruševac, Serbia
[2]Faculty of Technical Science, University of Priština, Kneza Miloša 7, 38220 Kosovska Mitrovica, Serbia
[3]Faculty of Technology and Metallurgy, University of Belgrade, Karnegijeva 4, 11120 Belgrade, Serbia
[4]Faculty of Science and Mathematics, University of Niš, Višegradska 33, 18000 Niš, Serbia

ABSTRACT

The removal of copper(II) ion from aqueous solution by the granular activated carbon, obtained from hazelnut shells (ACHS) (*Corylus avellana* L. var. *lunga istriana*), was investigated. The ACHS was prepared from ground dried hazelnut shells by specific method carbonisation and water steam activation at 950°C for 2 h. The granular activated carbon produced from hazelnut shells has a high specific surface area (1 452 $m^2 \cdot g^{-1}$) and highly developed microporous structure (micropore volume: 0.615 $cm^3 \cdot g^{-1}$). In batch tests, the influences of solution pH, contact time, initial metal ion concentration and temperature on the sorption of copper(II) ion on ACHS were studied. The results indicate that sorption of copper(II) ion on ACHS strongly depends on pH values. The adsorption data can be well described by the Langmuir isotherm and Redlich-Peterson model. The monolayer adsorption capacity of the ACHS-copper(II) ion, calculated from the Langmuir isotherms, is 3.07 $mmol \cdot g^{-1}$. The time-dependent adsorption of copper(II) ion could be described by the pseudo second-order and Elovich kinetics, indicating that the rate-limiting step might be a chemical reaction. The intra-particle diffusion model indicates that adsorption of copper(II) ions on ACHS was diffusion controlled.

Keywords: Activated carbon, *lunga istriana*, copper, equilibrium, kinetics

INTRODUCTION

Materials of highly porous structure are widely used as adsorbents in industrial separation processes. These materials presently have a very important role in the purification of industrial wastewater for removal of heavy metals, coloured and other organic pollutants. A large number of works on this topic are available in the scientific literature. Generally, all of this research can be divided into two groups: first, those which use raw materials, with or without purification, of relatively small specific area; second, those dealing with thermally-treated raw materials, which therefore have different degrees of carbonisation.

A wide variety of raw materials have been used: aerobic activated sludge, sulphurised activated carbon prepared from nut shells, wheat bran, valonia tannin resin, spent tea leaves, etc. (Orozco et al., 2007; Nouri et al., 2007; Tajar et al., 2009; Sengil et al., 2009; Bajpai and Jain, 2010). In addition, different methods of thermal treatment and the subsequent processing (activation) produce adsorbents with different properties (El Qada et al., 2008). Obviously, structural and adsorption characteristics of these materials depend on the nature of raw material and methods of subsequent processing. Shells of various stone fruits are very suitable for production of adsorbents with favourable adsorption properties. Recently there has been growing interest in hazelnut shell, which has exceptional morphological characteristics suitable for the production of a high quality adsorbent.

This paper deals with the adsorption properties of active carbon obtained from the hazelnut shell, the specific regional variety *lunga istriana*, grown in the central part of Serbia (region Šumadija). Hazelnut shell was obtained from food industry waste. The aim was to investigate the use of hazelnut shell waste for wastewater treatment. Active carbon of hazelnut shell was prepared by specific carbonisation method and activated by water steam. High temperature carbonisation and activation (950°C) of purified shell for an extended time of 2 h was applied. Influence of experimental conditions, such as pH value, initial copper(II) ion concentration and temperature, on adsorption behaviour was investigated.

EXPERIMENTAL

Materials and methods of activation

Hazelnut (*Corylus avellana* L. var. *lunga istriana*) shell was harvested from the central part of Serbia. Raw hazelnut shell was washed several times with deionised water in order to remove surface impurities and dried at 100°C overnight. Afterward, dried material was crushed by a hammer mill, simultaneously carbonised and activated at 950°C for 2 h by water steam, in a rotating cylindrical oven. The temperature at the entrance to the rotary oven was 150°C and 950°C at exit. Activated material was washed 3 times with distilled water, dried at 110°C for 24 h and stored in desiccators. Copper(II) acetate (CuAc), analytical reagent grade, was purchased from Merck, Inc. Deionised water (18 MΩ·cm resistivity) was used to prepare aqueous solutions of CuAc.

Methods of characterisation of ACHS

Scanning electron microscopy (SEM) was performed on a

JEOL JSM-6700 electron microscope. X-ray diffraction (XRD) data were obtained using a Bruker D8 Advance with Vario 1 focusing primary monochromator (Cu k_{a1} radiation, λ = 1.5405 ×10^{-10} m). Recording was done in the field of 2θ = 5° to 70° with the step of 0.025°C, time τ = 1 s. For the characterisation of diffractograms, the database diffraction ICDD (International Centre for Diffraction Data 1996) was used. The specific surface area, pore specific volume and pore diameter were measured by nitrogen adsorption/desorption at 77.4 K using a Micromeritics ASAP 2020MP.

Batch adsorption experiments

Batch equilibrium adsorption experiments were performed by varying the initial copper(II) ions concentration in the range from 13 mmol·ℓ$^{-1}$ to 260 mmol·ℓ$^{-1}$, at constant temperature. An Erlenmeyer flask (250 mℓ), fixed on a swinger (90 oscillations per minute), was used as an adsorption vessel, containing 100 mℓ copper(II) ion solution and 1.0 g of the adsorbent. After reaching adsorption equilibrium (6 h) all samples were centrifuged (1 500 r·min^{-1} for 5 min) to ensure separation of adsorbent particles. The adsorbed amount of copper(II) ions was calculated from the difference between initial and equilibrium Cu(II) ion concentration, as given by Eq. (1)

$$q = \frac{(C_o - C) \cdot V}{m_{ACHS}} \qquad (1)$$

where:

q is the mass of copper(II) ion adsorbed at time τ per unit mass of adsorbent

C_0 and C are the initial copper(II) ion concentration and the copper(II) ion concentration at appropriate time τ, respectively

V is the volume of CuAc solution (100 mℓ)

m_{ACHS} is the amount of adsorbent (1.0 g).

For each sample, the copper(II) ion concentration was measured in triplicate and the mean value was reported. The sorption of copper(II) on the Erlenmeyer flask surface, without sorbent addition, was negligible. Atomic absorption spectroscopy measurements of copper(II) ion concentrations were performed on a Perkin Elmer 1100B.

The influence of pH

In order to evaluate influence of pH on copper(II) sorption, the pH was varied in the range from 3.04 to 5.50, by adjustment with 0.01 mol·ℓ$^{-1}$ NaOH and 0.01 mol·ℓ$^{-1}$ HCl, at 25 ± 0.2°C. The optimal pH was found to be 5.0, and this pH was then used throughout all of the adsorption experiments. Initial concentration of copper(II) ion was 155 mmol·ℓ$^{-1}$. After reaching adsorption equilibrium (6 h) a sample was centrifuged (1 500 r·min^{-1} for 5 min), following by copper(II) determination in supernatant solution.

The influence of temperature

Influence of temperature on adsorption of copper(II) ion was studied for the temperature range from 20°C to 80°C. Starting concentration of copper(II) ion and pH was 255 mmol·ℓ$^{-1}$ and 5.0 ± 0.01, respectively.

Kinetic experiments

The effect of ACHS-copper(II) ion contact time was examined in the range 1 min to 6 h. In the kinetics experiments initial

TABLE 1
Physico-chemical properties of ACHS

Characteristics	Method (ASTM International, 2012; Beuth Verlag, 2012)	Value	
Specific surface area (m²·g⁻¹)	ASTM D 6556 - 10	1 452	
Iodine number (mg·g⁻¹)	ASTM D 4607	1 396	
Methylene blue index (mℓ)	ASTM C 837-09	19	
pH value	ASTM D 3838	9.1	
Ash (%)	ASTM D 2866	6.6	
Damp (%)	ASTM D 2867	8.3	
Bulk density (g·ℓ⁻¹)	ASTM D 2854	485	
Granular structure (%)	DIN 4188	> 1.6 mm	3.1
		1–1.6 mm	70.0
		0.5–1.0 mm	26.1
		<0.5 mm	0.9
Pore volume (mℓ·g⁻¹)	ASTM D4404 - 10	Micropore	0.615
		Mesopore	0.592
		Macropore	0.258

copper(II) ion concentration was 255 mmol·ℓ$^{-1}$. The residual copper(II) ion concentration in the liquid phase was periodically measured during the adsorption by an ion-selective electrode (type GPE 201.801, IHTM, Belgrade, Serbia).

RESULTS AND DISCUSSION

Characterisation of granular activated carbon

The ACHS is prepared from hazelnut shell by carbonisation and steam activation at 950°C for 2 h. ACHS characterisation was performed using standard methods (Table 1; ASTM International, 2012; Beuth Verlag, 2012), and, according to particle size and SEM analysis, the prepared active carbon was granular. The specific surface area and iodine number were 1 452 m²·g^{-1} and 1 396 mg·g^{-1}, respectively, which are the highest values thus far reported for activated carbon obtained from hazelnut shell. Alkali (Sayan, 2006), acid-treated (Demirbas et al., 2004) and salt-impregnated (ZnCl$_2$) (Aygün et al., 2003) active carbons have been reported to have specific surface areas of 10.1 m²·g^{-1}; 441 m²·g^{-1}and 793 m²·g^{-1}, respectively, while the specific surface areas of non-impregnated activated carbons were 825 m²·g^{-1} (Yalcin and Arol, 2002) and 786 m²·g^{-1} (Kazemipour et al., 2008). Therefore, applied long-term carbonisation/activation processes, at elevated temperature, do have significant influences on the development of high surface area and porosity of ACHS (Table 1).

In Fig. 1, an X-ray diffraction (XRD) micrograph of an ACHS surface is presented. In the observed spectra a peak at 2θ ≈ 25° originates from the amorphous structure of carbon (Allaf et al., 2011). A different full width at half-maximum (FWHM) value of the 002 peak, indicating the presence of a different micropore wall structure, can also be observed.
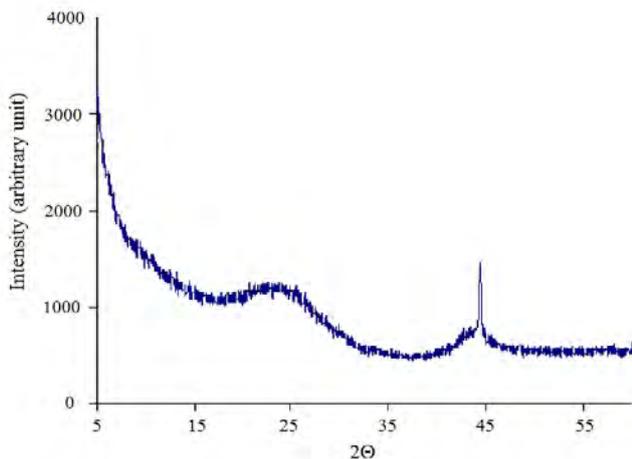
Figure 1
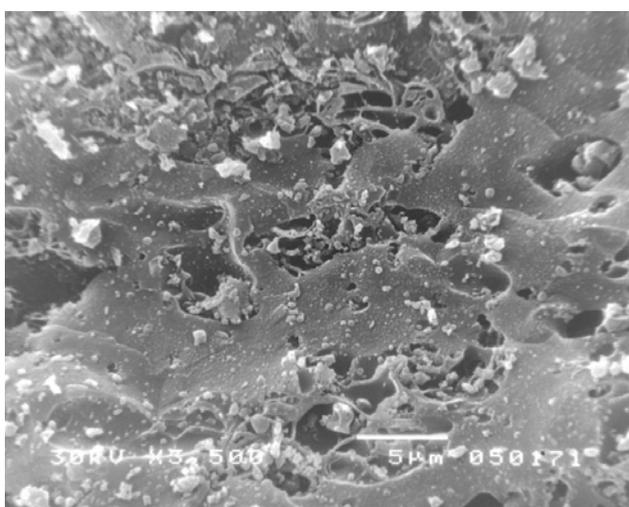*X-ray diffraction (XRD) profile of ACHS surface*

Figure 2
SEM photograph of ACHS, at 3 500 x magnification

A peak at $2\theta = 44.33°$ and interplanar distance $d = 2.0418 \times 10^{-10}$ m results from the crystal lattice of iron present in the carrier sample.

Scanning electron microscopy (SEM) is a technique which can be used for the study of active carbon morphology (Mohanty, 2006). Figure 2 shows the SEM photographs, at 3 500 times magnification, of the hazelnut shell after carbonisation at the optimum operating condition. The large surface-area of activated carbon is revealed, and pores of different sizes and shapes can be observed. Cavities resulting from the evaporation of volatile organic compounds produced during carbonisation are observed. Some particles and degradation products could be trapped in the pores and possibly block the entrances to meso- and micropores. For this reason, water steam activation could be considered to increase porosity, and thus contribute to significantly increased adsorption capacity of the ACHS.

Equilibrium time

The removal of copper(II) ion from aqueous solution by ACHS at pH 5.0 as a function of contact time indicates that sorption of copper(II) ion is a slow process; 6 h was sufficient for the
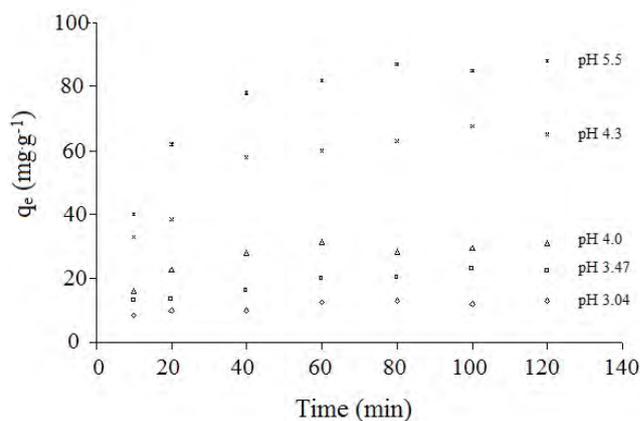

Figure 3
The influence of pH on adsorption capacity of copper(II) ions on ACHS, at 25°C and initial copper concentration of 255 mmol·ℓ⁻¹

sorption equilibrium to be achieved. Adsorption time was fixed at 6 h in subsequent adsorption experiments.

Effect of pH

pH is an important parameter influencing heavy metal adsorption from aqueous solutions. It affects both the surface charge of the adsorbent and the degree of ionisation of the heavy metal in solution. The copper(II) cations in aqueous solution at different pH values give rise to soluble ionic forms or more and less insoluble products, due to hydrolysis. The dominant species of copper(II) ion in the pH range 3 to 4 are copper(II) ion and $CuOH^+$, while the copper(II) ion at pH higher than 5.0 precipitates out as insoluble $Cu(OH)_2$ (Antunes, 2003).

A significant effect of pH on copper(II) sorption on ACHS (Fig. 3) was demonstrated, using 255 mmol ℓ⁻¹ initial copper(II) ion concentration. A gradual increase in pH causes ACHS adsorption capacity to increase; optimum pH was found to be 5.0 (q_e = 88.9 mg·g⁻¹). At pH < 5, the dominant copper species is Cu^{2+}, therefore, the lower Cu^{2+} sorption at low pH can be attributed mostly to the competition between H^+ and Cu^{2+} ion. A decrease in ACHS adsorption capacity at pH values higher than 5, is a consequence of an increase in Cu(II) hydroxy species, which have a lower affinity towards the ACHS surface. At pH higher than 6, precipitation of copper(II) hydroxide begins as a concurrent process (Antunes, 2003).

Effect of temperature

Temperature has a significant impact on the sorption process, resulting in varying contributions of individual sorption mechanisms to the overall process, involving the co-existence of physisorption, i.e., ion exchange, electrostatic attraction and chemisorption, i.e., surface complexation. Seven characteristics which determine the adsorption mechanism, i.e., chemisorption or physical adsorption, are described in the literature. Generally, chemisorption is favoured at increased temperature, and the opposite is true for physisorption (Sawalha et al., 2007).

The influence of temperature on ACHS sorption capacity is presented on Fig. 4, for the temperature range 20°C to 80°C, and at 255 mmol·ℓ⁻¹ initial copper(II) ion concentration. The removal of copper(II) ion increases in the temperature range 20°C to 60°C, and then starts decreasing rapidly at higher
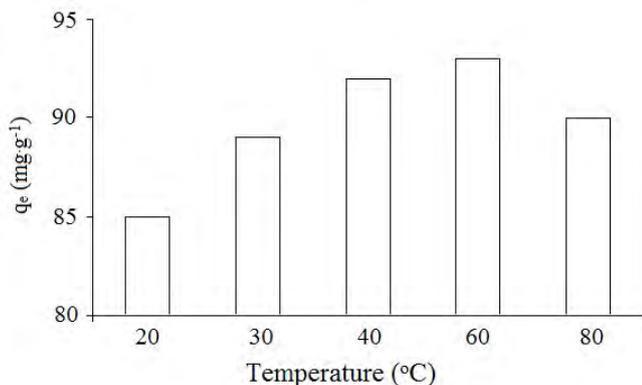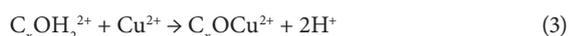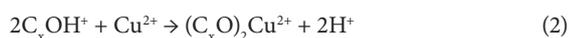
Figure 4
The influence of temperature on adsorption capacity for copper(II) ions on ACHS, at 25°C and initial copper concentration of 255 mmol·ℓ⁻¹

Figure 5
Adsorption isotherm for copper(II) ions on ACHS at 25°C

temperatures. Maximum sorption capacity, q_e = 93 mg·g⁻¹, was obtained at 60°C. At higher temperatures adsorption capacity decreases, most likely due to desorption being the more favoured process. Because of the complexity of the copper(II) sorption process, unequivocal evidence of the sorption mechanism will require additional and more detailed investigation.

Adsorption mechanism

Generally, it is expected that copper(II) ions are able to attach on adsorbent particle surfaces both physically (via adsorption by Van der Waals, electrostatic or London dispersion forces) and chemically (via a chemical complexation). In both cases, intra-particle diffusion of copper(II) ions will occur and additionally complicate the removal process. Although, a pure carbon surface is considered to be non-polar, some carbon-oxygen complexes (C_xO, CO_x, and C_xO_2) are usually present, which hydrolyse water molecules. Products of hydrolysis can react with copper(II) ions present in aqueous solution as shown in Eqs. (2) and (3) (Periasamy and Namasivayam, 1996):

$$2C_xOH^+ + Cu^{2+} \rightarrow (C_xO)_2Cu^{2+} + 2H^+ \qquad (2)$$

$$C_xOH_2^{2+} + Cu^{2+} \rightarrow C_xOCu^{2+} + 2H^+ \qquad (3)$$

The contribution of the proposed adsorption mechanisms presented in Eqs. (2) and (3) requires investigation in further kinetic studies, which could help in understanding the rate-determining step of the overall process.

Adsorption isotherms

In general, sorption processes were found to be complex, consisting of different steps such as external mass transfer of solute, boundary layer diffusion, intra-particle diffusion and adsorption at the active centres. Unless extensive experimental data are available, it is impossible to determine the rate-determining step of the overall process. However, sorption isotherm equations, which explain the process at equilibrium conditions, provide some quantitative information on sorption process, the surface properties and sorbent affinity. In addition, isotherm equations do not consider the complex mechanisms (external mass transfer, pore diffusion, chelation, ion exchange and chemisorption) involved in the sorption process; scientists use the equilibrium equation for ease of design of sorption systems.
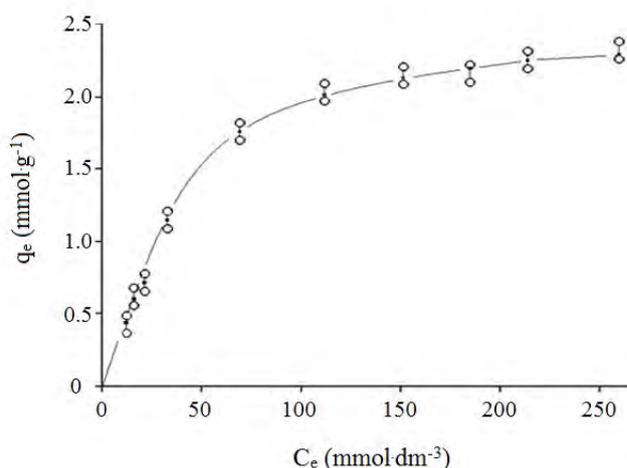
TABLE 2
Adsorption isotherms

Isotherm	Integral form	Linear form
Freundlich	$q_e = K_F C_e^{b_F}$	$\ln q_e = \ln K_F + b_F \ln C_e$
Langmuir	$q_e = \dfrac{K_L C_e}{1 + a_L C_e}$	$\dfrac{C_e}{q_e} = \dfrac{1}{K_L} + \dfrac{a_L}{K_L} C_e$
Redlich-Peterson	$q_e = \dfrac{K_{RP} C_e}{1 + a_{RP} C_e^{b_{RP}}}$	$\dfrac{C_e}{q_e} = \dfrac{1}{K_{RP}} + \dfrac{a_{RP}}{K_{RP}} C_e^{b_{RP}}$

Some of the isotherm equations that could describe solid–liquid adsorption systems are Langmuir, Freundlcih, Sips, Toth isotherm, Redlich–Peterson, Dubinin–Raduskevich and Harins–Jura isotherm equations (Ho et al., 2002). Among of them, Langmuir (Langmuir, 1916), Freundlich (Freundlich, 1906), and Redlich–Peterson (Redlich and Peterson, 1959) isotherms are the most commonly used (Altenora et al., 2009).

The adsorption data for copper(II) ion on ACHS is shown in Fig. 5., which is in agreement with the standard isotherm, Type 1 of the Brunauer, Deming, Deming and Teller classification (Brunauer et al., 1940). In the initial part of the curve, at low copper concentrations, the ratio of ACHS functional sites, which participate in sorption, to Cu(II) ions is relatively high, resulting in an efficient and fast sorption process. At higher concentrations of the solute, the change in ACHS sorption capacity, q_e, with increasing Cu(II) concentration is smaller, until maximum sorption capacity is reached. This type of curve is characteristic of high-porosity adsorbents, which is in accordance with the data presented in Table 1, as micro- and meso-pores make up 82.3% of the total pore volume.

Freundlich model

The integral and linear form of the Freundlich model adsorption isotherm (Freundlich, 1906) is presented in Table 2. The Freundlich isotherm assumes a heterogeneous surface with a non-uniform distribution of heat of adsorption and multilayer adsorption over the surface. When an adsorption process is well described by the Freundlich model, the calculated K_F parameter is proportional to capacity and b_F to intensity of adsorption.

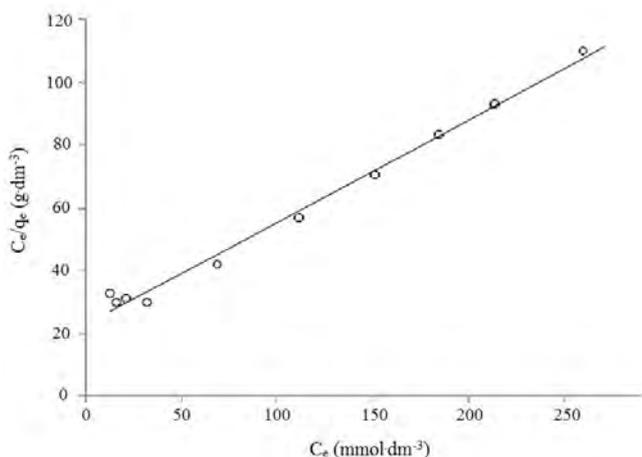In this study, Freundlich constants were obtained by fitting

Figure 6
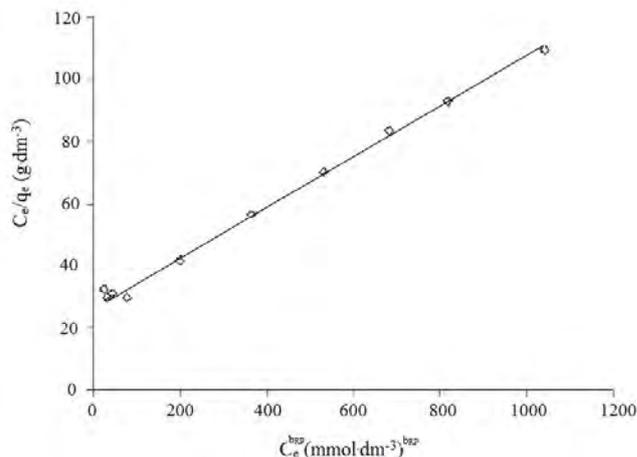*Linear form of the Langmuir model adsorption isotherm for copper(II) ions on ACHS at 25°C*

Figure 7
Linear form of the Redlich-Peterson model adsorption isotherm for copper(II) ions on ACHS, at 25°C

TABLE 3 Freundlich, Langmuir and Redlich-Peterson isotherm parameters for copper(II) sorption on ACHS					
Freundlich		**Langmuir**		**Radlich-Peterson**	
K_F (mmol·g⁻¹)/ (mmol·ℓ⁻¹)^{bF}	0.118	K_L (ℓ·g⁻¹)	0.044	K_{RP} (ℓ·g⁻¹)	0.0370
b_F	0.531	a_L (ℓ·mmol⁻¹)	0.014	a_{RP} (ℓ·mmol⁻¹)^{bRP}	0.00298
		q_m (mmol·g⁻¹)	3.070	b_{RP}	1.250
R^2	0.941	R^2	0.990	R^2	0.996
RMS (%)	±15.3	RMS (%)	±8.4	RMS (%)	±5.4

the adsorption equilibrium data to the isotherm models, and are listed in Table 3. As there was some deviation of the experimental data from the linear form of the Freundlich adsorption isotherm this suggests that this model is not a good description of copper(II) ion sorption on ACHS, as indicated by the relatively low value of R^2 and high value of RMS (±15.3) (Table 3).

Langmuir model

The integral and linear form of the Langmuir model adsorption isotherm (Langmuir, 1916) is presented in Table 2. This is the most widely used adsorption model, which assumes the following: monolayer adsorption; adsorption takes place at specific homogeneous sites within the adsorbent, and no further adsorption can take place at that site; adsorption energy is constant and does not depend on the degree of occupation of an adsorbent's active centres; the strength of the intermolecular attractive forces is believed to fall off rapidly with distance; the adsorbent has a finite capacity for the dye (at equilibrium, a saturation point is reached where no further adsorption can occur); all sites are identical and energetically equivalent; the adsorbent is structurally homogeneous; there is no interaction between molecules adsorbed on neighbouring sites.

In this study Langmuir constants were obtained by fitting the adsorption equilibrium data to the isotherm models (Fig. 6.); these are listed in Table 3. The R^2 values (Table 3) for

the Langmuir model are higher, and RMS values are lower, than those for the Freundlich model. This indicates that the Langmuir model better describes the adsorption of copper(II) ion onto ACHS, with a somewhat better fit at the higher concentration of copper(II) ion, of 50 mmol·g⁻¹. Such results indicate a more homogeneous distribution of active sites on the ACHS surface and thus homogenous coverage by adsorbate, relative to copper(II) ion removal by raw hazelnut shells (Demirbas et al., 2008).

The maximum adsorption capacity for copper(II) ion from aqueous solution by ACHS is 3.07 mmol·g⁻¹ (195 mg·g⁻¹) (Langmuir model). Periasamy and Namasivayam (1996) reported the sorption capacity for copper(II) ion on active carbon obtained from peanut shell (Langmuir model) is 65.57 mg·g⁻¹. The higher value for ACHS obtained in this study can be attributed to the greater specific surface area and pore volume of the ACHS.

Redlich-Peterson model

Table 2 presents the integral and linear form of the Redlich-Peterson model (Redlich and Peterson, 1959). Redlich and Peterson have proposed an empirical equation incorporating three parameters more appropriate for the description of adsorption equilibrium over a wide range of concentrations (El Qada et al., 2008), which can be applied either in homogenous or heterogeneous systems. This isotherm combines elements from both the Langmuir and Freundlich equations, and the mechanism of adsorption proposed is a hybrid process, which does not follow ideal monolayer adsorption. The Redlich-Peterson equation is reduced to the Freundlich isotherm at low surface coverage and to the Langmuir isotherm at high adsorbate concentration.

In this study, Redlich-Peterson constants were obtained by fitting the adsorption equilibrium data to the isotherm models (Fig. 7.); these are listed in Table 3. It can be seen that the value of b_{RP} tends to 1 (1.25), indicating that the applied model indeed approaches the Langmuir model. Values in Table 3 show that the maximum sorption capacity, q_m, is larger than values reported previously. Based on the correlation coefficient (R^2 = 0.996) and RMS (± 5.4%), the Redlich-Peterson model best describes the sorption process.

Adsorption kinetics

The removal of copper(II) ions by ACHS as a function of contact time was analysed by pseudo second-order, Elovich and intra-particle diffusion kinetic models. Kinetic studies have been performed to investigate the sorption mechanism, which is helpful for selecting optimum operating conditions for the full-scale batch process.

Pseudo second-order model

The pseudo second-order equation was used to correlate experimental data based on the proposed adsorption mechanism (Cheung et al., 2001):

$$2M_{(sol)} + Cu^{2+}_{(aq)} \rightarrow M_2Cu^{2+}_{(ads.\ phase)} \tag{10}$$
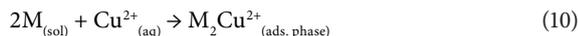
The corresponding pseudo second-order kinetic rate equation is expressed as:

$$\frac{dq_\tau}{d\tau} = k_2(q_e - q_\tau)^2 \tag{11}$$

where:

q_e (mmol·g⁻¹) and q_τ (mmol·g⁻¹) are the sorption capacity at equilibrium and at appropriate time τ (min), respectively constant k_2 (g·mmol⁻¹·min⁻¹) is the pseudo second-order rate constant.

For the boundary conditions $\tau = 0 \rightarrow q_\tau = 0$ at $\tau = \tau_o \rightarrow q_\tau = q$; the integrated form of Eq. (11) becomes:

$$q_\tau = \frac{k_2 q_e^2 \tau}{1 + k_2 q_e \tau} \tag{12}$$

and its linearised form:

$$\frac{\tau}{q_\tau} = \frac{1}{k_2 q_e^2} + \frac{1}{q_e}\tau \tag{13}$$

The initial sorption rate, h, at $\tau = 0$ is defined as:

$$h = k_2 q_e^2 \tag{14}$$

and half-adsorption time of the copper(II) ions $t_{1/2}$, is:

$$\tau_{1/2} = \frac{1}{k_2 q_e} \tag{15}$$

The plot of τ/q_τ against τ of Eq. (13) gave a linear relationship, and q_e and k_2 were determined from the slope and intercept of the plot (Fig. 8). Kinetic and statistical parameters of the pseudo-second-order model for the adsorption of copper(II) ion on ACHS are shown in Table 4. Among the three kinetic models, the pseudo-second-order model gave the best fit of
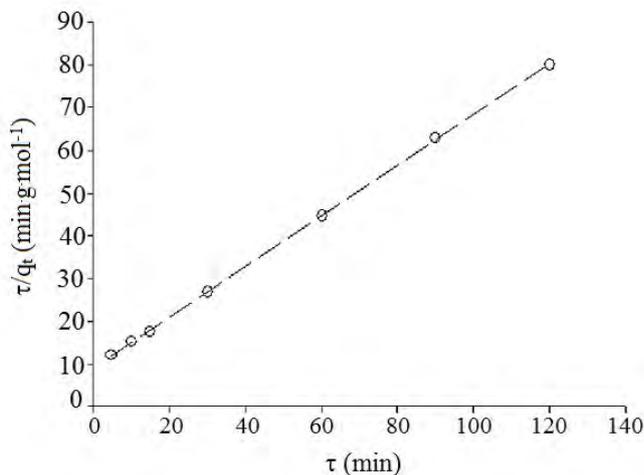

Figure 8
Linear form of the pseudo-second-order kinetic model for copper(II) ions on ACHS at 25°C

experimental data, having the highest correlation coefficient ($R^2 = 0.999$), and the lowest normalised root mean square value RMS (0.82%). According to some authors (Ho, 2003; Bulut and Tez, 2007), this result indicates a high prevalence of chemisorption in the overall sorption process.

Elovich model

The Elovich equation has been applied satisfactorily to some chemisorption data and has been found to cover a large range of slow adsorption processes (Feng-Chin et al., 2009). The Elovich equation is often valid for systems in which the adsorbing surface is heterogeneous. The equation is stated as:

$$\frac{dq_\tau}{d\tau} = a_E \cdot e^{-b_E q_\tau} \tag{16}$$

or in integrated form:

$$q_\tau = \frac{1}{b_E}\ln(a_E b_E) + \frac{1}{b_E}\ln(\tau + \tau_o) \tag{17}$$

where:

a_E (mmol·g⁻¹·min⁻¹) is the initial adsorption rate
b_E (g·mmol⁻¹) is the desorption constant during only one experiment

Teng and Hsieh (1999) proposed that the constant a_E is related to the rate of chemisorption and the constant b_E is related to the surface coverage. The parameter τ_o (2.14 min) was

TABLE 4						
Parameters and statistical data of kinetic models						
Pseudo-second order		**Elovich**		**Intra-particle diffusion model**		
				First stage		**Second stage**
k_2 (g·mmol⁻¹·min⁻¹)	0.0396	a_E (mmol·g⁻¹·min⁻¹)	0.184	$k_{p,1}$ (min⁻¹)	0.210	$k_{p,2}$ (min⁻¹)	0.0496
q_e (mmol·g⁻¹)	1.681	b_E (g·mmol⁻¹)	2.601			C_I	0.9579
h (mmol·g⁻¹·min⁻¹)	0.112	τ_o (min)	2.140				
$T_{1/2}$ (min)	15.02						
R^2	0.999	R^2	0.992	R^2_1	0.993	R^2_1	0.999
RMS (%)	±0.82	RMS (%)	±4.58	RMS (%)	±3.6	RMS (%)	±0.22

estimated by trial and error, to obtain a linear plot of q_τ against $\ln(\tau_+\tau_o)$; a_E and b_E are calculated from the intercept and the slope. According to Eq. (17), for $\tau_o = 0$ at $\tau = 0$, time constant τ_o can be calculated from Eq. (18):

$$\tau_o = \frac{1}{a_E b_E} \tag{18}$$

The linear form of Eq. (17), on the basis of experimental data for the adsorption of copper(II) ions on ACHS, is shown in Fig. 9. The Elovich model parameters are shown in Table 3, confirming that the experimental kinetic data give a good fit to this equation and similar results previously published (Ho and McKay, 2000). The values of Elovich model parameters a_E and b_E are 0.184 mmol·g^{-1}·min^{-1} and 2.090 g·mmol^{-1}, respectively, as previously found for similar systems (Cheung et al., 2001). Time constant τ_o, calculated according to Eq. (18) ($\tau_o = 2.09$ min) is close to the value calculated using the trial-and-error method ($\tau_o = 2.14$ min; error ±2.3%).

Intra-particle diffusion model

Adsorptive transfer from solution to adsorbent surface is highly complex. The most commonly used model for analysing the overall adsorption process is the intra-particle diffusion model, given by the following equation (Weber and Morris, 1963):

$$q_\tau = K_d \cdot \sqrt{\tau} + C_I \tag{19}$$

where:
q_τ is amount of metal adsorbed at time τ (mmol·g^{-1})
K_d is the intra-particle diffusion rate constant (mmol·g^{-1}·min$^{0.5}$)
C_I is the intercept (mmol·g^{-1}).

If intra-particle diffusion occurs then q_τ against $\sqrt{\tau}$ will be linear and the line will pass through the origin, indicating that intra-particle diffusion was the only rate-limiting parameter controlling the process. Otherwise, some other mechanism is also involved. The value of the intercept gives an indication of the thickness of the boundary layer, i.e., the larger the intercept the greater is the boundary layer effect (Kannan and Sundaram, 2001).

In Fig. 10, a plot of adsorbed Cu(II) per unit mass of ACHS adsorbent, qt vs. $t^{0.5}$, is presented; this indicates that the intra-particle diffusion model well describes the adsorption process. Two linear consecutive regions could be observed: Part (I), fast uptake, is attributed to intra-particle diffusion; and Part (II) is a slower process indicating the effect of pore diffusion, which could be attributed to the difference in rates of mass transfer in the initial and final stages of adsorption (Panday et al., 1986). This is attributed to the instantaneous adsorbate bonding at the most readily available adsorbing sites on ACHS. It is noteworthy that in Part (I) the line passes through the origin, indicating that the process is predominantly controlled by intra-particle diffusion, rather than film diffusion. Part (II) may be attributed to a slower diffusion of the adsorbate from the surface film into the meso- and micro-pores, which are less accessible sites of adsorption. This also stimulates a very slow rate of migration of adsorbate from the liquid phase on to the adsorbent surface. The values of $k_{p,1}$ and $k_{p,2}$, as obtained from the slopes of the straight lines, are given in Table 4, and the data indicate that pore diffusion is not the sole rate-controlling step (Mane et al., 2007).
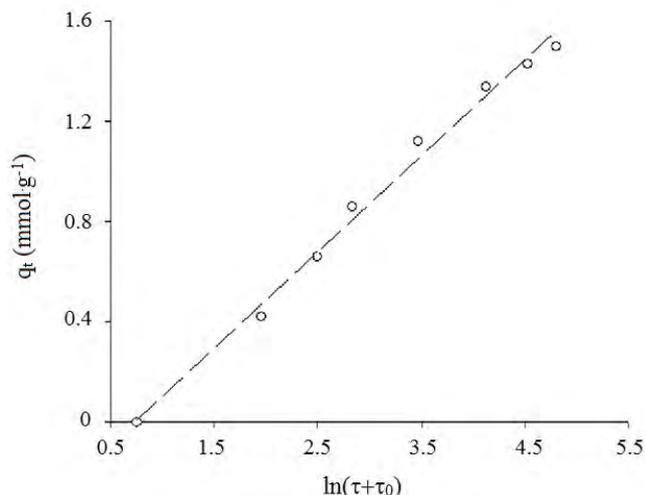
Figure 9
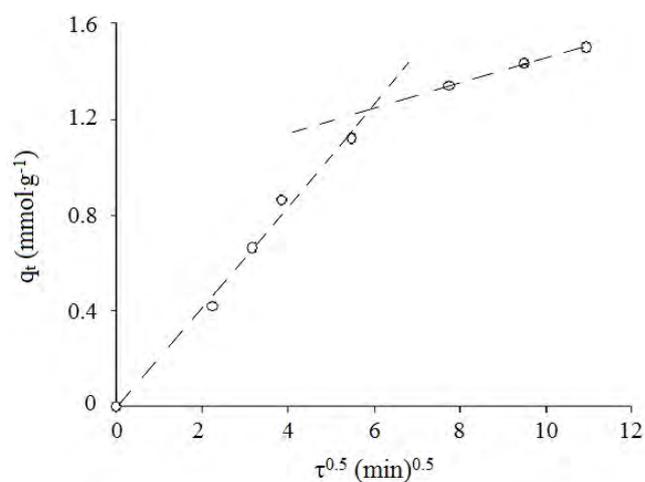*Linear form of the Elovich kinetic model for copper(II) ions on ACHS, at 25°C*

Figure 10
Linear form of the intraparticle diffusion model for copper(II) ions on ACHS, at 25°C

CONCLUSION

The granular activated carbon, ACHS, produced from hazelnut shells has a high specific surface area and highly developed meso- and micro-porous structure. The specific method of carbonisation and activation applied in this study favours the formation of meso- and micro-porous structure in ACHS. The sorption experimental data for copper(II) ion on ACHS follow the Langmuir and Radlich-Peterson adsorption isotherm models. The highest value of R^2 and lowest value of normalised RMS are obtained using the Radlich-Peterson model. The kinetics of copper(II) ion removal on ACHS follow the pseudo-second-order model, indicating that chemical adsorption between the adsorbent and the adsorbate prevails rather than physical adsorption. As the intra-particle diffusion model fits the kinetic data well, adsorption of copper(II) ions on the granular activated carbon is also diffusion controlled. The prepared ACHS can be used as an effective adsorbent for batch adsorption of copper(II) ion from aqueous solution.

ACKNOWLEDGEMENTS

REFERENCES

ALLAF RM, RIVERO IV, SPEARMAN SS and HOPE-WEEKS LJ (2011) On the preparation of As-produced and purified single-walled carbon nanotube samples for standardized X-ray diffraction character. *Mater. Charact.* **62** 857–864.

ALTENORA S, CARENEA B, EMMANUELB E, LAMBERT J, EHR-HARDTC JJ and GASPARDA S (2009) Adsorption studies of methylene blue and phenol onto vetiver roots activated carbon prepared by chemical activation. *J. Hazardous Mater.* **165** 1029–1039.

ANTUNES WM, LUNA AS, HENRIQUES CA and COSTA AC (2003) An evaluation of copper biosorption by a brown seaweed under optimized conditions. *Electron. J. Biotechnol.* **6** 174–184.

ASTM INTERNATIONAL (2012) URL: http://www.astm.org/Standard/index.shtml.

AYGÜN A, YENISOY-KARAKAS S and DUMAN I (2003) Production of granular activated carbon from fruit stones and nutshells and evaluation of their physical, chemical and adsorption properties. *Micropor. Mesopor.* **66** 189–195.

BAJPAI SK and JAIN A (2010) Removal of copper(II) from aqueous solution using spent tea leaves (STL) as a potential sorbent. *Water SA* **36** 221–228.

BEUTH VERLAG (2012) URL: http://www.beuth.de/en

BRUNAUER S, DEMING LS and DEMING TELLER WS (1940) Types of adsorption isotherms. *J. Am. Chem. Soc.* **62** 1723.

BULUT Y and TEZ Z (2007) Adsorption studies on ground shells of hazelnut and almond. *J. Hazardous Mater.* **149** 35–41.

CHEUNG CW, PORTER JF and McKAY G (2001) Sorption kinetic analysis for the removal of cadmium ions from effluents using bone char. *Water Res.* **35** 605–612.

DEMIRBAS Ö, KARADAĞ A, ALKAN M, DOĞAN M, BULUT Y and TEZ Z (2008) Removal of copper ions from aqueous solutions by hazelnut shell. *J. Hazardous Mater.* **153** 677–648.

FENG-CHIN W, RU-LING T and RUEY-SHIN J (2009) Characteristics of Elovich equation used for the analysis of adsorption kinetics in dye-chitosan systems. *Chem. Eng. J.* **150** 366–373.

FREUNDLICH HMF (1906) Über die adsorption in lösungen. *Z. Phys. Chem.* **57A** 385–470.

HO YS, McKAY G (2004) Sorption of copper(II) from aqueous solution by peat. *Water Air Soil Pollut.* **158** 77–97.

HO YS, PORTER JF and McKAY G (2002) Equilibrium isotherm studies for the sorption of divalent metal ions onto peat: Copper, nickel and lead, single component systems. *Water Air Soil Pollut.* **141** 1–33.

KANNAN K and SUNDARAM MM (2001) Kinetics and mechanism of removal of methylene blue by adsorption on various carbons – A comparative study. *Dyes Pigments* **51** 25–40.

KAZEMIPOUR M, ANSARI M, TAJROBEHKAR S, MAJDZADEH M and KERMANI HR (2008) Removal of lead, cadmium, zinc, and copper from industrial wastewater by carbon developed from walnut, hazelnut, almond, pistachio shell, and apricot stone. *J. Hazardous Mater.* **150** 322–327.

LANGMUIR I (1916) The constitution and fundamental properties of solids and liquids. *J. Am. Chem. Soc.* **38** 2221–2295.

MANE VS, MALL ID and SRIVASTAVA VC (2007) Use of bagasse fly ash as an adsorbent for the removal of brilliant green dye from aqueous solution. *Dyes Pigments* **73** 269–278.

MOHANTY K (2006) Preparation and characterization of activated carbons from *Sterculia alata* nutshell by chemical activation with zinc chloride to remove phenol from wastewater. *Adsorption* **12** 119–132.

NOURI L, GHODBANE I, HAMDAOUI O and CHIHA M (2007) Batch sorption dynamics and equilibrium for for the removal of cadmium ion from aqueous phase using wheat bran. *J. Hazardous Mater.* **149** 115–125.

OROZCO MF, CONTRERAS EM, BERTOLA N and ZARITZKY N (2007) Hexavalent chromium removal using aerobic activated sludge. *Water SA* **33** 239–244.

PANDAY KK, PRASAD G and SINGH VN (1986) Mixed adsorbent for Cu(II) removal from aqueous solutions. *Environ. Technol. Lett.* **50** (7) 547–554.

PERIASAMY K and NAMASIVAYAM C (1996) Removal of copper(II) by adsorption onto peanut hull carbon from water and copper plating industry wastewater. *Chemosphere* **32** 769–789.

EL QADA EN, ALLEN SJ and WALKER GM (2008) Adsorption of basic dyes from aqueous solution onto activated carbons. *Chem. Eng. J.* **135** 174–184.

REDLICH O and PETERSON DL (1959) A useful adsorption isotherm. *J. Phys. Chem.* **63** 1024.

SAWALHA MF, PERALTA-VIDEA JR, ROMERO-GONZALEZ J, DUARTE-GARDEA M, GARDEA-TORRESDEY JL (2007) Thermodynamic and isotherm studies of the biosorption of Cu(II), Pb(II) and Zn(II) by leaves of saltbush. *J. Chem. Thermodynamics* **39** 488–492.

ŞAYAN E (2006) Ultrasound-assisted preparation of activated carbon from alkaline impregnated hazelnut shell: An optimization study on removal of Cu(II) from aqueous solution. *Chem. Eng. J.* **115** 213–218.

SENGIL I, OZACAR M and TURKMENLER H (2009) Kinetic and isotherm studies of Cu(II) biosorption onto valonia tannin resin. *J. Hazardous Mater.* **162** 1046–1052.

TAJAR AF, KAGHAZCHI T and SOLEIMANI M (2009) Adsorption of cadmium from aqueous solutions on sulfurized activated carbon prepared from nut shells. *J. Hazardous Mater.* **165** 1159–1164.

TENG H and HSIEH C (1999) Activation energy for oxygen chemisorption on carbon at low temperatures. *Ind. Eng. Chem. Res.* **38** 292–297.

WEBER WJ and MORRIS JC (1963) Kinetics of adsorption on carbon from solution. *Am. Soc. Civ. Eng.* **89** (SA2) 1–40.

YALCIN M and AROL AI (2002) Gold cyanide adsorption characteristics of activated carbon of non-coconut shell origin. *Hydrometallurgy* **63** 201–206.